J Therm Anal Calorim
DOI 10.1007/s10973-017-6807-1

The isobaric heat capacities and thermodynamic properties of ionic liquid 1-ethylpyridinium bis(trifluoromethylsulfonyl)imide

Ling Zheng[1] · Long Li[2] · Ya-Fei Guo[2] · Wei Guan[1] · Da-Wei Fang[1]

Received: 16 July 2017 / Accepted: 29 October 2017

Abstract Ionic liquid 1-ethylpyridinium bis(trifluoromethylsulfonyl)imide ($[C_2py][NTf_2]$) was synthesized and characterized by ^1H NMR spectroscopy, ^{13}C NMR spectroscopy and thermal gravity analysis. The molar heat capacities of $[C_2py][NTf_2]$ were measured using a heat-flow calorimeter with "3D Calvet" calorimetric sensor from (293 to 312) K. The experiment value of molar heat capacity 502.15 J K^{-1} mol^{-1} at 298.15 K was obtained. Moreover, the estimation values of molar heat capacity were calculated by using 4 methods at 298.15 K, and the result showed the Paulechka et al.'s method was more appropriate for predicting the molar heat capacity of IL $[C_2py][NTf_2]$, and the error was less than 2%. In addition, the freezing point T^* was calculated by freezing point depression, which was approximately equal to experimental value 305.08 K. The molar enthalpy of fusion $\Delta_f H_m = 26.77$ kJ mol^{-1}, molar melting entropy $\Delta_{de}S_m = 90.60$ J mol^{-1} K^{-1} and the freezing constant K_f were also calculated.

Keywords Ionic liquid · Molar heat capacity · Molar enthalpy · Adiabatic calorimetry · Thermodynamic property

Introduction

Ionic liquids (ILs) are known as "green solvents" due to their great capacity and their "environmentally friendly" properties in comparison with common organic solvents [1–3]. The capability of ILs to be used as solvents for the desulfurization of fuels has been tested [4–8] and considered promising agents for gas separation as they show a great variety in the ability to absorb gases during last years [9, 10]. Ionic liquid with anion of bis(trifluoromethylsulfonyl)imide also has an application prospect as solvent to extract benzene from alkanes [11]. Moreover, during the practical application of ionic liquids, thermal management of industrial processes is very important for safety production and reducing energy consumption, so heat capacity of ILs is indispensable basic data.

The low-temperature heat-flow calorimeter BT2.15 from Setaram with "3D Calvet" calorimetric sensor can be used to determine the heat capacity [12–14], which compared with traditional differential scanning calorimetry (DSC) with 2D flat sensors, the sensor has a novel structure, and the sample was surrounded by multiple layers of sensors; it means all the heat flow was captured for both sample and reference pool, rather than just detected the heat changes in bottom of the crucible, in which the premise was the sample plate contacted with the sensor closely. In addition, Zhang et al. [15]. reported the uncertainty of the heat capacity measurements did not exceed 0.01 by using BT2.15, and the average relative deviation was found to be 0.33%, and the maximum relative deviation was 0.79% in

Electronic supplementary material The online version of this article (https://doi.org/10.1007/s10973-017-6807-1) contains supplementary material, which is available to authorized users.

✉ Wei Guan
guanweiy@sina.com

✉ Da-Wei Fang
davidfine@163.com

[1] College of Chemistry, Liaoning University, Shenyang 110036, People's Republic of China

[2] Tianjin Key Laboratory of Marine Resources and Chemistry, College of Chemical Engineering and Material Sciences, Tianjin University of Science and Technology, Tianjin 300457, People's Republic of China

Published online: 13 November 2017

the accuracy of the measurement. However, the calculated standard uncertainties were ± 1 K for the temperature in the thermal analysis and ± 5% for the determination of the molar heat capacity when using a differential scanning calorimeter according to Gómez et al.'s report [16]. That is BT2.15 has a higher accuracy in determination of the heat capacity than DSC.

As a continuation of our investigation [17–20], in this paper, the IL [C2py][NTf2] was synthesized and the molar heat capacities in temperature range of (293–312) K were measured using a heat-flow calorimeter with "3D Calvet" calorimetric sensor. The value of molar heat capacity at 298.15 K was calculated by polynomial fitting equation. The molar enthalpy of fusion $\Delta_f H_m$ and molar melting entropy $\Delta_{de} S_m$ were also calculated.

Experimental

Preparation of IL [C_2py][NTf_2]

[C_2py][Br] (*N*-Alkylpyridinium bromide) was synthesized according to Tong et al.'s report [21]. IL [C_2py][NTf_2] (1-Ethylpyridinium bis(trifluoromethylsulfonyl)imide) was synthesized by using the ion exchange reaction from [C_2py][Br] and $HN(SO_2CF_3)_2$ (bis(trifluoromethanesulfonyl)imide) in distilled water and stirred for 3 h at room temperature. The product was washed several times with distilled water until no Br^- was indicated by the solution of $AgNO_3/HNO_3$. The final product was dried in vacuum for 2 days at 353 K. Structure of the resulting [C_2py][NTf_2] was confirmed by ^{1}H NMR, ^{13}C NMR spectroscopy and thermal gravity analysis (TGA) (see Figures S1, S2 and S3 in Supporting Information). The ^{1}H NMR (600 MHz, $CDCl_3$, δ): 9.77 (d, 1H, N–CH), 8.49 (t, 1H, CH–CH–CH), 8.01 (t, 2H, CH–CH–N), 4.61 (m, 2H, CH_2–CH_3), 1.63 (t, 3H, N–CH_3). From ^{1}H NMR and ^{13}C NMR spectroscopy, impurity peaks were not found. TGA spectroscopy showed a mass loss peak of IL [C_2py][NTf_2]. In addition, water content was measured using a Karl Fischer moisture titrator (ZSD-2 type) before measurement for three times (81, 85 and 82 ppm) which are all less than 85 ppm.

Calorimeter calibration

The molar heat capacity, C_p, was determined using a heat-flow calorimeter BT2.15 from Setaram, which adopts "3D Calvet" calorimetric sensor with resolution 0.1 μW, the accuracy of temperature measurement is ± 0.01 K, and the mass is with an uncertainty of ± 0.00001 g. The calorimeter was performed calibration with the standard molar heat capacity of KCl (purity > 99.95%) at 298.15 K and repeated for seven times. The results were 0.687333, 0.688046, 0.687966, 0.687269, 0.688009, 0.687719 and 0.687580 J K^{-1} g^{-1}, respectively. The relative standard deviation *RSD* was 0.066%, which compared with 0.6879 J K^{-1} g^{-1} [22] are within the limit.

The heat capacities measurement of the IL

In this experiment, the test temperature was firstly set to 293 K and remain for 5 h, then heat to 312 K with a heating rate of 0.02 K min^{-1} under nitrogen environment. In this condition, the heat flow signals (experimental before-after) are at a same height.

Results and discussion

Measurement of molar heat capacity

The experimental isobaric heat capacities of [C_2py][NTf_2] with a temperature step of 0.1 K are given in Table 1; by plotting molar heat capacity C_p/J mol^{-1} K^{-1} against temperature *T*/K, the curve with r^2 exceeding 0.999 was obtained (see Fig. 1). Figure 1 shows the melting process with a sharp endothermic peak from 299 to 308 K; the melting point was determined to be 305.08 ± 0.05 K, which compared with 303.65 K [23] was approximately equal. The experimental values of the molar heat capacity were fitted before and after the melting process according to the following polynomial equations:

$$\text{From 293 to 299 K}: C_p/\text{J K}^{-1}\,\text{mol}^{-1} = 449.5564 + 46.5024X + 13.3862X^2 + 22.8571X^3 \quad (1)$$

$$\text{From 299 to 305 K}: C_p/\text{J K}^{-1}\,\text{mol}^{-1} = 1081.04 + 1281.88X + 1361.77X^2 + 2595.12X^3 + 6696.64X^4 + 5984.04X^5 - 2538.25X^6 - 5518.05X^7 - 1706.07X^8 \quad (2)$$

$$\text{From 305 to 308 K}: C_p/\text{J K}^{-1}\,\text{mol}^{-1} = 1223.09 - 4496.34X + 9655.65X^2 - 2519.79X^3 - 9337.44X^4 + 2667.32X^5 + 3377.35X^6 \quad (3)$$

$$\text{From 308 to 312 K}: C_p/\text{J K}^{-1}\,\text{mol}^{-1} = 474.32 + 0.82906X + 0.44134X^2 - 0.27295X^3 - 0.70171X^4 + 0.20361X^5 + 0.58283X^6 \quad (4)$$

where *X* is the reduced temperature, $X = [T - (T_{max} + T_{min})/2]/[(T_{max} - T_{min})/2]$; *T* is the experimental temperature;

Table 1 Experimental molar heat capacity, C_p/J K^{-1} mol^{-1}, versus temperature, T/K of IL [C_2py][NTf_2], at the pressure, $p = 0.1$ Mpa

T/K	C_p/J K^{-1} mol^{-1}	T/K	C_p/J K^{-1} mol^{-1}	T/K	C_p/J K^{-1} mol^{-1}	T/K	C_p/J K^{-1} mol^{-1}
292.981	394.5121	299.331	562.7867	305.399	7993.3415	308.762	473.9394
293.138	395.7844	299.412	568.6033	305.434	7708.7617	308.840	473.9449
293.183	397.1257	299.493	574.6340	305.477	7403.5183	308.852	473.9670
293.241	398.3886	299.577	580.9363	305.520	7078.6625	308.881	473.9701
293.301	400.1093	299.655	587.6760	305.559	6741.1837	308.920	473.9829
293.364	401.6407	299.730	594.6578	305.598	6389.7097	308.960	473.9942
293.423	403.1946	299.807	602.0359	305.632	6029.0855	309.043	474.0031
293.489	404.8117	299.891	609.9267	305.675	5659.5444	309.082	474.0066
293.551	406.4640	299.964	617.9193	305.717	5288.2063	309.127	474.0136
293.617	407.9963	300.047	626.3153	305.752	4912.8065	309.166	474.0209
293.683	409.6507	300.122	635.1987	305.832	4538.2632	309.240	474.0415
293.759	411.1683	300.207	644.7180	305.843	4168.1403	309.271	474.0508
293.828	412.7473	300.283	654.4784	305.888	3803.2887	309.307	474.0539
293.897	414.4387	300.366	664.9807	305.925	3449.5974	309.318	474.0846
293.967	415.9823	300.450	675.5203	305.967	3102.7741	309.345	474.1199
294.040	417.6782	300.529	686.9487	306.003	2769.4442	309.387	474.1323
294.113	419.2426	300.603	698.8217	306.043	2450.8556	309.423	474.1525
294.187	420.5838	300.684	711.1271	306.084	2152.4330	309.462	474.1571
294.260	422.4213	300.766	724.0104	306.129	1883.7275	309.506	474.1579
294.333	423.7413	300.846	737.7907	306.177	1656.5143	309.541	474.2037
294.417	425.3090	300.923	752.0370	306.216	1448.7647	309.583	474.2048
294.487	426.5063	301.004	766.8903	306.252	1276.1237	309.625	474.2196
294.563	427.9144	301.087	782.5438	306.294	1137.8935	309.666	474.2262
294.640	429.0827	301.169	799.0857	306.331	1042.2236	309.707	474.2270
294.713	430.3707	301.247	816.6333	306.379	959.3273	309.748	474.2390
294.793	431.5369	301.321	835.1887	306.417	872.9017	309.785	474.2417
294.874	432.4841	301.402	854.7506	306.451	819.6967	309.823	474.2530
294.952	433.6753	301.489	875.6047	306.497	781.2651	309.869	474.2611
295.025	434.8547	301.568	898.0383	306.533	751.9683	309.906	474.2661
295.103	436.0787	301.647	921.3650	306.577	721.6026	309.941	474.2902
295.187	437.2061	301.722	946.9903	306.613	694.1133	309.983	474.2968
295.266	438.3217	301.801	974.2550	306.652	671.5007	310.023	474.3573
295.341	439.6263	301.886	1003.0987	306.691	651.4887	310.067	474.3577
295.420	440.7810	301.963	1034.5987	306.740	632.4330	310.110	474.3585
295.494	441.9824	302.042	1068.5066	306.781	615.4493	310.143	474.3600
295.578	443.1992	302.123	1105.4013	306.820	599.8177	310.187	474.3616
295.657	444.5392	302.209	1144.8817	306.862	585.6473	310.223	474.4198
295.733	445.7236	302.287	1188.1885	306.940	572.5167	310.264	474.4276
295.813	447.0540	302.364	1235.6307	306.951	566.6629	310.303	474.4373
295.891	448.4487	302.447	1286.8053	306.981	555.3523	310.347	474.4912
295.976	449.8012	302.523	1342.6255	307.020	545.0564	310.383	474.4920
296.053	451.1177	302.604	1403.8083	307.065	535.6702	310.423	474.5001
296.131	452.3238	302.684	1467.1470	307.108	527.0497	310.467	474.5059
296.213	453.8497	302.767	1540.3243	307.140	519.1007	310.508	474.5505
296.294	455.2703	302.847	1620.8253	307.183	508.4536	310.547	474.5537
296.373	456.6330	302.925	1707.9787	307.223	502.0330	310.585	474.5614
296.456	458.0733	303.024	1804.7033	307.263	494.8379	310.605	474.5668
296.537	459.5717	303.082	1911.4383	307.330	478.0748	310.641	474.6413

Table 1 continued

T/K	C_p/J K^{-1} mol^{-1}	T/K	C_p/J K^{-1} mol^{-1}	T/K	C_p/J K^{-1} mol^{-1}	T/K	C_p/J K^{-1} mol^{-1}
296.611	461.1828	303.160	2029.2547	307.372	475.2134	310.682	474.6561
296.693	462.7051	303.242	2159.0397	307.419	474.1055	310.721	474.6794
296.770	464.3540	303.320	2302.9403	307.454	473.0019	310.762	474.6867
296.851	465.9347	303.397	2464.2327	307.491	472.6804	310.844	474.6922
296.932	467.6950	303.475	2645.2863	307.536	473.2158	310.853	474.7092
297.011	469.3723	303.557	2850.1220	307.578	473.6605	310.881	474.7263
297.092	471.2890	303.635	3082.8043	307.611	473.7361	310.924	474.7310
297.173	473.0746	303.713	3339.5771	307.655	473.7656	310.963	474.8086
297.253	475.0104	303.791	3620.8195	307.694	473.7885	311.044	474.8350
297.337	477.0221	303.876	3928.0883	307.732	473.8052	311.085	474.8361
297.417	479.0697	303.955	4262.2846	307.776	473.8180	311.128	474.8443
297.496	481.0467	304.037	4620.8053	307.816	473.8211	311.169	474.8881
297.572	483.3359	304.110	4999.5034	307.854	473.8285	311.201	474.9063
297.653	485.6164	304.179	5393.6827	307.892	473.8405	311.244	474.9067
297.731	487.9497	304.271	5812.9382	307.933	473.8494	311.288	474.9184
297.841	490.3720	304.347	6246.6447	307.973	473.8533	311.323	474.9234
297.892	492.7477	304.423	6671.1083	308.010	473.8584	311.366	474.9312
297.973	495.4810	304.508	7082.8475	308.051	473.8591	311.415	474.9393
298.050	498.3247	304.583	7493.6641	308.093	473.8591	311.449	475.0371
298.132	501.3073	304.668	7888.9193	308.135	473.8669	311.488	475.0549
298.212	504.0967	304.741	8258.9497	308.177	473.8684	311.524	475.0619
298.289	507.3590	304.822	8580.2173	308.218	473.8696	311.561	475.0643
298.357	510.4863	304.897	8846.5518	308.252	473.8715	311.608	475.0743
298.425	513.9347	304.963	9038.7637	308.294	473.8816	311.642	475.0751
298.553	517.4980	304.997	9156.0626	308.363	473.8844	311.681	475.0980
298.641	521.1741	305.047	9235.8052	308.376	473.8921	311.698	475.1201
298.696	525.0130	305.082	9264.5373	308.417	473.8964	311.719	475.1364
298.778	528.9677	305.122	9237.4827	308.454	473.8968	311.764	475.1477
298.857	533.0953	305.165	9152.6120	308.493	473.9022	311.793	475.1624
298.933	537.6053	305.197	9036.7736	308.561	473.9026	311.817	475.1927
299.017	542.1408	305.240	8887.5517	308.645	473.9131	311.841	475.2121
299.096	546.9740	305.277	8706.5863	308.674	473.9169	311.887	475.2276
299.173	551.9355	305.315	8496.0650	308.687	473.9286	311.921	475.3033
299.257	557.3107	305.353	8256.6773	308.728	473.9360	312.083	475.4930

T_{max} and T_{min} are the maximum and minimum of the temperature in the experimental temperature range. The correlation coefficient *r*-square of the four fittings is all above 0.999. Then, the value of molar heat capacity, $C_{p,m} = 502.15 \pm 0.33$ J K^{-1} mol^{-1}, at 298.15 K was calculated by the polynomial Eq. (1).

Estimation of molar heat capacity

The molar heat capacity of IL [C_2py][NTf_2] was estimated by using 4 methods. According to Paulechka et al.'s report, [24] molar heat capacity can be estimated using the molar volume (V/cm^3 mol^{-1}) through the following empirical equation:

$$C_p(\text{cal.1}) = 8.6 + 1.915\,V \quad (5)$$

where $V = 252.55$ cm^3 mol^{-1} (298.15 K), which was calculated by using the equation, $V = M/\rho$, $\rho = 1.5375$ g cm^{-3} [23], the estimated value of C_p(cal.1) = 492.23 J K^{-1} mol^{-1} for [C_2py][NTf_2] obtained from Eq. (5). Besides, according to the gene expression programming (GEP) model [25], the prediction of experimental heat capacity data can be estimated by using the operators of −, + and × . The mathematical formula is as follows:

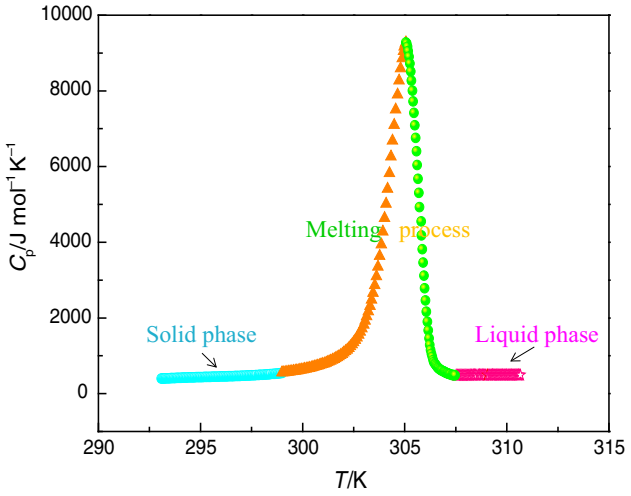

Fig. 1 Plot of C_p versus T of IL [C_2py][NTf_2]

Table 2 Values of molar heat capacity of estimated and experiment at 298.15 K

	C_p (cal.1)	C_p (cal.2)	C_p (cal.3)	C_p (cal.4)	C_p (exp.)
C_p/J K^{-1} mol^{-1}	492.23	293.50	477.50	433.69	502.15
RD/%	1.97	41.55	4.91	13.63	

$$\begin{aligned} C_p(\text{cal.2}) = {} & 0.610577(T) + 3.2299289(\text{N-c}) \\ & + 7.999972(\text{N-a}) + 0.638975(\text{Mw}) \\ & + 16.965817(\text{Cc}) - 0.159172(T) \\ & \times (\text{CH}_3\text{R} - c) - 170.658909 \end{aligned} \quad (6)$$

where T is temperature, C_C is number of carbon atoms in cation part of IL, number of atoms of anion part (N-a), M_W is molecular weight of IL, (N-c) is number of atoms of cation part and (CH_3R-c) is number of methyl groups in cation counter parts, and C_p(cal.2) = 293.50 J K^{-1} mol^{-1} (298.15 K) was calculated. Farahani et al. [26] also reported that it can be calculated by following formula:

$$\begin{aligned} C_p(\text{cal.3}) = {} & -122.16826 + 0.45794T \\ & + 12.8395\text{N}_C - 56.85424\text{CH}_3\text{R}_C \\ & + 19.25836\text{N}_a - 11.36109n\text{H}_a \end{aligned} \quad (7)$$

where N_C = number of atoms of cation, N_a = number of atoms of anion, CH_3R_C = number of methyl groups in cation counter parts, nH_a = number of hydrogen atoms in anion, T = temperature; then, C_p(cal.3) = 477.50 J K^{-1} mol^{-1} (298.15 K) was obtained. Ahmadi et al. [27] also put forward a formula, by which the molar heat capacity can be estimated through the numbers of atoms including C, N, S, O, F, Br, Cl and B:

$$\begin{aligned} C_p(\text{cal.4}) = {} & 0.2808T^{1.0854} - 17.5066\ln(T) + 0.6593M_W^{1.0793} \\ & + 15.9932C_A + 16.1292C_C - 2.8956\text{N} - 11.7667\text{S} \\ & - 1.3729\text{O} - 4.1977(\text{F} + \text{Br} + \text{Cl}) + 6.7438\text{B} - 12.399 \end{aligned} \quad (8)$$

where T = temperature; M_W = molecular weight of IL; C_A = number of carbon atoms of anion; C_C = number of carbon atoms of cation; N, S, O, F, Br, Cl and B = number of nitrogen, sulfur, oxygen, fluorine, bromine, chlorine and boron atoms of IL, C_p(cal.4) = 433.69 J K^{-1} mol^{-1} (298.15 K) was also calculated. The values of molar heat capacity for 4 estimating methods and experiment are all listed in Table 2.

As shown in Table 2, the estimated value calculated from Paulechka et al.'s method is the nearest when compared with the experiment, and the error is less than 2%. According to Benito et al.'s report [28], the heat capacity determined by DSC was 523 J K^{-1} mol^{-1}, which is higher than our experiment and the error was more than 4% when compared with the estimated value 492.23 J K^{-1} mol^{-1} and the experimental value 502.15 J K^{-1} mol^{-1}. The deviation of experimental data may be caused by the different efficiencies of the instrument sensors. That is, the Paulechka et al.'s method which is based on the molar volume is more appropriate for predicting the molar heat capacity of IL [C_2py][NTf_2].

The molar enthalpy of fusion

The molar enthalpy of fusion of IL [C_2py][NTf_2], $\Delta_f H_m$, can be obtained from the following equation:

$$\Delta_f H_m = \left[Q - n \int_{T_i}^{T_{de}} C_{p(i)} \mathrm{d}T - n \int_{T_{de}}^{T_f} C_{P(f)} \mathrm{d}T - \int_{T_i}^{T_f} H_0 \mathrm{d}T \right] / n \quad (9)$$

where n is the amount of substance, T_{de} is the temperature of solid–liquid phase transition (peak melting temperature), T_i is the temperature at which the solid–liquid phase transition started, T_f is the temperature at which the solid–liquid phase transition ended, Q is total heat including sample and pool from T_i to T_f, $C_{p(i)}$ is molar heat capacity at T_i, $C_{p(f)}$ is the molar heat capacity at T_f, H_0 is molar heat capacity ($T_i - T_f$). The molar enthalpy of fusion $\Delta_f H_m$ of IL was obtained using Eq. (9). The value of $\Delta_f H_m$ = 26.77 kJ mol^{-1} is bigger than 22.44, 6.83 and 5.90 kJ mol^{-1} for [C_2py][PF_6], [C_3py][PF_6] and [C_5py][PF_6] [27], respectively. It may because the higher relative molecular mass and volume need more heat from solid to liquid.

Determination of melting point by freezing point depression

The trace impurities can also make a difference for the experimental result even the purity of 99 mass% is high. In that case, IL can be taken as a dilute solution which consists of solvent and impurity. Since the freezing point of dilute solution is certain to below the melting point of pure IL, then freezing point depression equation was obtained according to phase equilibrium principle as follows:

$$\ln x_A = \Delta_f H_m (T_{de} - T^*)/RT_{de}T^* \quad (10)$$

where x_A is molar fraction, T^* is melting point of pure IL, R is Avogadro constant. Since $T_{de}T^* \approx T_{de}^2$, then Eq. (10) was rearranged:

$$T^* = T_{de} - RT_{de}^2 \ln x_A/\Delta_f H_m \quad (11)$$

From Eq. (11), the value of $T^* = 306.48$ K was obtained, which compared with the average 305.08 K was a little bigger. The reason was caused by trace water in ionic liquid [C_2py][NTf_2].

The molar melting entropy $\Delta_{de}S_m$ of IL can also be calculated according to melting point of pure IL:

$$\Delta_{de}S_m = \Delta_f H_m/T^* \quad (12)$$

From Eq. (12), $\Delta_{de}S_m = 90.60 \pm 0.06$ J mol^{-1} K^{-1} was calculated, which compared with 60.04, 18.41 and 17.98 J mol^{-1} K^{-1} [27] for [C_2py][PF_6], [C_3py][PF_6] and [C_5py][PF_6], respectively, is bigger. Besides, the freezing constant K_f was also calculated by the following equation:

$$K_f = RT^{*2}M_A/\Delta_f H_m \quad (13)$$

where M_A is molar mass, then the freezing constant $K_f = 1.09 \times 10^4$ g mol^{-1} K^{-1} was calculated.

Conclusions

In this paper, IL [C_2py][NTf_2] was synthesized and characterized. The molar heat capacities of ionic liquid [C_2py][NTf_2] were measured using a calorimeter with "3D Calvet" calorimetric sensor from (293 to 312) K. The value of molar heat capacity 502.15 J K^{-1} mol^{-1} was obtained at 298.15 K. Moreover, the estimation values of molar heat capacity were calculated by using 4 methods at 298.15 K, and the result showed the estimating formula which based on the molar volume was more appropriate for predicting the molar heat capacity of IL [C_2py][NTf_2] with the error less than 2%. The molar enthalpy of fusion $\Delta_f H_m = 26.77$ kJ mol^{-1}, molar melting entropy $\Delta_{de}S_m = 90.60$ J mol^{-1} K^{-1} and the freezing constant K_f were also calculated.

Acknowledgements The project was supported by the National Natural Science Foundation of China (21373005, 21673107) and LNET (LR2015025).

References

1. Calvar N, Gómez E, Macedo EA, Domínguez Á. Thermal analysis and heat capacities of pyridinium and imidazolium ionic liquids. Thermochim Acta. 2013;565:178–82.
2. Rocha MAA, Bastos M, Coutinho JAP. Santos LMNBF. Heat capacities at 298.15 K of the extended [$C_nC_1$im][Ntf_2] ionic liquid series. J Chem Thermodyn. 2012;53:140–3.
3. Lin PY, Soriano AN, Leron RB, Li MH. Electrolytic conductivity and molar heat capacity of two aqueous solutions of ionic liquids at room-temperature: measurements and correlations. J Chem Thermodyn. 2010;42:994–8.
4. Bösmann A, Datsevich L, Jess A, Lauter A, Schmithz C, Wasserscheid P. Deep desulfurization of diesel fuel by extraction with ionic liquids. Chem Commun. 2001;23:2494–5.
5. Rodríguez-Cabo B, Francisco M, Soto A, Arce A. Hexyl dimethylpyridinium ionic liquids for desulfurization of fuels. Effect of the position of the alkyl side chains. Fluid Phase Equilib. 2012;314:107–12.
6. Arce A, Francisco M, Soto A. Evaluation of the polysubstituted pyridinium ionic liquid [hmmpy][Ntf_2] as a suitable solvent for desulfurization: phase equilibria. J Chem Thermodyn. 2010;42:712–8.
7. Gao HS, Li YG, Wu Y, Luo MF, Li Q, Xing JM, Liu HZ. Extractive desulfurization of fuel using 3-methylpyridinium-based ionic liquids. Energy Fuels. 2009;23:2690–4.
8. Verdía P, González EJ, Rodríguez-Cabo B, Tojo E. Synthesis and characterization of new polysubstituted pyridinium-based ionic liquids: application as solvents on desulfurization of fuel oils. Green Chem. 2011;13:2768–76.
9. Han XX, Armstrong DW. Ionic liquids in separations. Acc Chem Res. 2007;40:1079–86.
10. Raeissi S, Peters CJ. A potential ionic liquid for CO_2-separating gas membranes: selection and gas solubility studies. Green Chem. 2009;11:185–92.
11. Requejo PF, Calvar N, Domínguez Á, Gómez E. Comparative study of the LLE of the quaternary and ternary systems involving benzene, *n*-octane, *n*-decane and the ionic liquid [BMpyr][NTf_2]. J Chem Thermodyn. 2016;98:56–61.
12. Casás LM, Plantier F, Pineiro MM, Legido JL, Bessières D. Calibration of a low temperature calorimeter and application in the determination of isobaric heat capacity of 2-propanol. Thermochim Acta. 2010;507–508:123–6.
13. Casás LM, Legido JL, Pozo M, Mourelle L, Plantier F, Bessières D. Specific heat of mixtures of bentonitic clay with sea water or distilled water for their use in thermotherapy. Thermochim Acta. 2011;524:68–73.
14. Coulier Y, Ballerat-Busserolles K, Mesones J, Lowe A, Coxam J. Excess molar enthalpies and heat capacities of 2-methylpiperidine − water and *N*–methylpiperidine − water systems of low to moderate amine compositions. J Chem Eng Data. 2015;60:1563–71.
15. Dong L, Zheng D, Nie N, Li Y. Performance prediction of absorption refrigeration cycle based on the measurements of vapor pressure and heat capacity of H_2O + [DMIM]DMP system. Appl Energy. 2012;9:326–32.
16. Calvar N, Gómez E, Macedo EA, Domínguez Á. Thermal analysis and heat capacities of pyridinium and imidazolium ionic liquids. Thermochim Acta. 2013;565(565):178–82.

17. Wei J, Chang C, Zhang YY, Hou SY, Fang DW, Guan W. Prediction of thermophysical properties of novel ionic liquids based on serine [$C_n$mim][Ser] ($n = 3, 4$) using semiempirical methods. J Chem Thermodyn. 2015;90:310–6.
18. Ma XX, Wei J, Zhang QB, Tian F, Feng YY, Guan W. Prediction of thermophysical properties of acetate-based ionic liquids using semiempirical methods. Ind Eng Chem Res. 2013;52:9490–6.
19. Xing NN, Dai B, Ma XX, Wei J, Pan Y, Guan W. The molar surface Gibbs energy and prediction of surface tension of [$C_n$py][DCA] ($n = 3, 4, 5$). J Chem Thermodyn. 2016;95:21–5.
20. Wei J, Zhang QB, Tian F, Zheng L, Guan W, Yang JZ. Study on the thermodynamic properties for ionic liquid [C_6mim][OAc](1-hexyl-3-methylimidazolium acetate). Fluid Phase Equilib. 2014;371:1–5.
21. Tong B, Liu QS, Tan ZC, Welz-Biermann U. Thermochemistry of alkyl pyridinium bromide ionic liquids: calorimetric measurements and calculations. J Phys Chem A. 2010;114:3782–7.
22. Speight JG. Lange's handbook of chemistry. 16th ed. New York: McGraw-Hill; 2005.
23. Liu QS, Yang M, Yan PF, Liu XM, Tan ZC, Welz-Biermann U. Density and surface tension of ionic liquids [$C_n$py][NTf_2] ($n = 2, 4, 5$). J Chem Eng Data. 2010;55:4928–30.
24. Paulechka YU, Kabo AG, Blokhin AV, Kabo GJ, Shevelyova MP. Heat capacity of ionic liquids: experimental determination and correlations with molar volume. J Chem Eng Data. 2010;55:2719–24.
25. Barati-Harooni A, Najafi-Marghmaleki A, Arabloo M, Mohammadi AH. Chemical structural models for prediction of heat capacities of ionic liquids. J Mol Liq. 2017;232:113–22.
26. Farahani N, Gharagheizi F, Mirkhani SA, Tumba K. A simple correlation for prediction of heat capacities of ionic liquids. Fluid Phase Equilib. 2013;337:73–82.
27. Ahmadi A, Haghbakhsh R, Raeissi S, Hemmati V. A simple group contribution correlation for the prediction of ionic liquid heat capacities at different temperatures. Fluid Phase Equilib. 2015;403:95–103.
28. Benito J, Garcı´a-Mardones M, Pe´rez-Gregorio V, Gasco´n I, Lafuente C. Physicochemical study of *n*-ethylpyridinium bis(trifluoromethylsulfonyl)imide Ionic Liquid. J Solut Chem. 2014;43:696–710.